

10. The LAGEOS satellites are heavy brass and aluminum satellites, of about 406 kg, completely passive and covered with retroreflectors, orbiting about 6000 km above Earth's surface. LAGEOS, launched in 1976 by NASA, and LAGEOS II, launched by NASA and ASI in 1992, have an essentially identical structure but are in different orbits. The semimajor axis of LAGEOS is  $a_1 \approx 12,270$  km, the period  $P_1 \approx 3.758$  hours, the eccentricity  $e_1 \approx 0.004$ , and the inclination  $i_1 \approx 109.9^\circ$ . For LAGEOS II,  $a_{II} \approx 12,163$  km,  $e_{II} \approx 0.014$ , and  $i_{II} \approx 52.65^\circ$ .
11. *International Earth Rotation Service (IERS) Annual Report, 1996* (Observatoire de Paris, Paris, July 1997).
12. D. McCarthy, *The 1996 IERS Conventions* (Observatoire de Paris, Paris, 1996).
13. F. G. Lemoine *et al.*, presented at the 1997 Institute of Astronomy and Geophysics Scientific Assembly, Rio de Janeiro, Brazil, 5 to 9 September 1997.
14. D. P. Rubincam, *J. Geophys. Res.* **93**, 13803 (1988); *ibid.* **95**, 4881 (1990); \_\_\_\_\_ and A. Mallama, *ibid.* **100**, 20285 (1995); C. F. Martin and D. P. Rubincam, *ibid.* **101**, 3215 (1996).
15. P. Farinella, D. V. Y. Vokrouhlicky, F. Barlier, *ibid.*, 17861.
16. R. S. Gross, *ibid.*, p. 8729.
17. D. E. Pavlis *et al.*, *GEODYN II: Operations Manual* (1997), vol. 3.
18. I. Ciufolini, *Phys. Rev. Lett.* **56**, 278 (1986); *Nuovo Cimento A* **109**, 1709 (1996).
19. \_\_\_\_\_, *Int. J. Mod. Phys. A* **4**, 3083 (1989); see also B. Tapley, J. C. Ries, R. J. Eanes, M. M. Watkins, *NASA-ASI Study on LAGEOS III* (1989), part A, I. Ciufolini *et al.*; *ibid.*, part B.
20. I. Ciufolini *et al.*, *Classical Quantum Gravity* **14**, 2701 (1997).
21. This work was significantly aided by several programs and facilities of NASA Goddard Space Flight Center (GSFC), in particular through data provided to us by the Crustal Dynamics Data and Information System (CDDIS) of NASA GSFC and the use of the program GEODYN II. We also appreciate unconditional help from D. E. Pavlis and D. D. Rowlands. I.C. and F.C. were supported in part by ASI, E.F.-V. and J.P.-M. by the Ministries of Education and Defense of Spain, and E.P. in part by NASA grant NCC-5-60.

28 October 1997; accepted 12 February 1998

## Quantitation of HIV-1-Specific Cytotoxic T Lymphocytes and Plasma Load of Viral RNA

Graham S. Ogg, Xia Jin, Sebastian Bonhoeffer, P. Rod Dunbar, Martin A. Nowak, Simon Monard, Jeremy P. Segal, Yunzhen Cao, Sarah L. Rowland-Jones, Vincenzo Cerundolo, Arlene Hurley, Martin Markowitz, David D. Ho, Douglas F. Nixon, Andrew J. McMichael\*

Although cytotoxic T lymphocytes (CTLs) are thought to be involved in the control of human immunodeficiency virus-type 1 (HIV-1) infection, it has not been possible to demonstrate a direct relation between CTL activity and plasma RNA viral load. Human leukocyte antigen-peptide tetrameric complexes offer a specific means to directly quantitate circulating CTLs *ex vivo*. With the use of the tetrameric complexes, a significant inverse correlation was observed between HIV-specific CTL frequency and plasma RNA viral load. In contrast, no significant association was detected between the clearance rate of productively infected cells and frequency of HIV-specific CTLs. These data are consistent with a significant role for HIV-specific CTLs in the control of HIV infection and suggest a considerable cytopathic effect of the virus *in vivo*.

At all stages of disease, plasma RNA viral load remains the most potent predictor of outcome in HIV-1-infected individuals (1). Cross-sectional stratification of RNA loads provides a highly significant indicator of the likelihood of progression to acquired immunodeficiency syndrome (AIDS) and mortality (1). Even shortly after seroconversion the virological setpoint is significantly associated with prognosis, suggesting that in most individuals the determinants of progression are present early in the course of infection (1). The dominant host immunological factors involved in the control of

progression remain unresolved, but most infected individuals show a vigorous HIV-specific immune response comprising both cellular and humoral mechanisms.

Cytotoxic T lymphocytes (CTLs) are believed to be important in the control of HIV infection (2-6) because the emerging HIV-specific CTL response observed during primary infection follows a close temporal association with acute viral load reduction (2, 3). Evidence also comes from the characterization of virus mutants that escape recognition by CTLs that have been identified at seroconversion, during asymptomatic HIV infection, during AIDS, and after CTL immunotherapy (4, 5), suggesting that CTLs exert a considerable selective pressure at many stages of disease. In addition to killing infected cells, CD8<sup>+</sup> T cells effectively inhibit HIV replication *in vitro* through the production of chemokines (6).

Mathematical modeling of viral dynamics has predicted that if CTLs are important in the control of HIV infection, there should be an inverse association between HIV-specific CTL activity and plasma

RNA viral load (7, 8). However, previous studies have demonstrated no significant correlation between circulating HIV-specific CTL activity and plasma RNA viral load during the chronic phase (9-11). High CTL activity in the presence of low levels of plasma viral RNA has been reported, but these findings were based on qualitative associations and indirect assays of CTL function that require culture and expansion *in vitro* (12). In a study of early HIV infection only, the levels of Env-specific cultured memory CTLs were inversely correlated with RNA viral load, but this finding did not extend to Gag- or Pol-specific memory CTLs (13). Direct measurement of lytic activity by uncultured, circulating HIV-specific CTLs (effector CTLs, CTL<sub>E</sub>) has only been possible in a subset of patients because the assay is relatively insensitive, requiring antigen-specific CTL<sub>E</sub> frequencies above 1 in 100 peripheral blood mononuclear cells (PBMCs) for lysis to be detectable (14). Here we have used highly sensitive human leukocyte antigen (HLA)-tetrameric complexes for a cross-sectional analysis of HIV Gag- and Pol-specific CTL<sub>E</sub> frequencies from 14 untreated HLA A\*0201-positive individuals at different stages of infection.

HLA-tetrameric complexes can be used to directly visualize antigen-specific T cells by flow cytometry (15). HLA heavy chain is expressed in *Escherichia coli* with an engineered COOH-terminal signal sequence containing a biotinylation site for the enzyme BirA (16). After refolding of heavy chain,  $\beta_2$ -microglobulin ( $\beta_2M$ ), and peptide, the complex is biotinylated and tetramer formation induced by the addition of streptavidin. By means of fluorescently labeled streptavidin, the tetramer can be used to stain and sort antigen-specific cells. The staining is highly specific such that CTL clones and lines directed to different epitope peptides bound to the same HLA molecule do not stain (15). Figure 1, A to C, shows examples of HLA-tetrameric staining with (A) HLA B\*3501 tetramer refolded around the envelope peptide DPN-PQEVVL [Env(77-85)] (17), (B) HLA

G. S. Ogg, P. R. Dunbar, S. L. Rowland-Jones, V. Cerundolo, A. J. McMichael, Institute of Molecular Medicine, Nuffield Department of Medicine, Oxford OX3 9DS, UK. X. Jin, S. Monard, J. P. Segal, Y. Cao, A. Hurley, M. Markowitz, D. D. Ho, D. F. Nixon, Aaron Diamond AIDS Research Center, 455 First Avenue, New York, NY 10016, USA.

S. Bonhoeffer, Aaron Diamond AIDS Research Center, 455 First Avenue, New York, NY 10016, USA, and Department of Zoology, University of Oxford, South Parks Road, Oxford OX13PS, UK.

M. A. Nowak, Department of Zoology, University of Oxford, South Parks Road, Oxford OX1 3PS, UK.

\*To whom correspondence should be addressed.

A\*0201 tetramer refolded around the Gag peptide SLYNTVATL [Gag(77–85)] (18), and (C) HLA A\*0201 tetramer refolded around the Pol peptide ILKEPVHGV [Pol(476–484)] (19, 20). Using freshly isolated PBMCs, we characterized epitope-specific cytolytic activity with 86 <sup>51</sup>Cr-release cytotoxic assays, each performed in triplicate, and compared the results to HLA-tetrameric complex staining (Fig. 1D). Extending previous data (15), we found a highly significant positive correlation ( $P < 0.001$ ) between fresh cytolysis and tetramer staining. Low levels of cytolysis (<5%) previously discounted as below an empirical limit in other studies may in fact reflect significant numbers of circulating epitope-specific CTLs. By means of two-color staining, we were able to accurately detect tetramer-positive cells at levels as low as 0.02% of CD8<sup>+</sup> T lymphocytes. Direct sorting of tetramer-stained PBMCs into Elispot plates (21) is a very rapid and reliable protocol that can be applied to establish the specificity of low-frequency CTL responses, such as tumor-specific CTL responses in patients with melanoma (15).

To address the sensitivity of tetramer binding, we performed a parallel experiment using an HLA A\*0201 influenza A matrix peptide GILGFVFTL (residues 58 to 66) tetramer to sort stained cells from a source population of 0.04% of CD8<sup>+</sup> T lymphocytes derived from an HLA A\*0201-positive donor. When duplicate sets of tetramer-positive cells were placed directly into Elispot wells, every cell could be accounted for after influenza matrix-specific interferon- $\gamma$  (IFN- $\gamma$ ) production was determined (21). In contrast, CD8<sup>+</sup> T cells that did not stain with the influenza A matrix tetramer were unable to produce IFN- $\gamma$  in response to peptide-specific stimulation. Tetramer-positive cells were also plated directly into cloning wells (22), and after 3 weeks in culture all expanded clones were able to secrete IFN- $\gamma$  when exposed to HLA A\*0201-matched target cells coated with the influenza A matrix peptide (22). Therefore, staining of PBMCs with HLA-tetrameric complexes provides a highly sensitive and specific method for detecting antigen-specific CTLs.

At least 66% of HLA A\*0201-positive individuals have circulating CTLs that recognize Gag(77–85), an A\*0201-restricted Gag epitope. Most (70%) of those individuals that do not recognize the A2Gag epitope will recognize Pol(476–484), an A\*0201-restricted Pol epitope, so that the addition of both the A2Gag and A2Pol responses gives a representation of total A\*0201-directed CTL activity (23). Using HLA-tetrameric complexes, we compared the percentage of uncultured CD8<sup>+</sup> T cells specific for the A2Gag epitope with plasma RNA viral

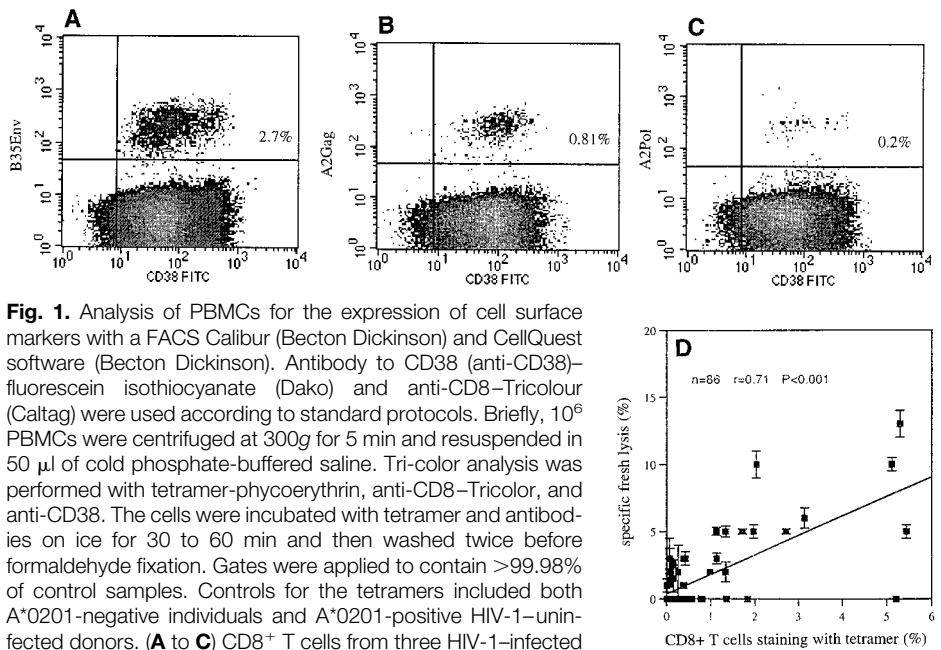
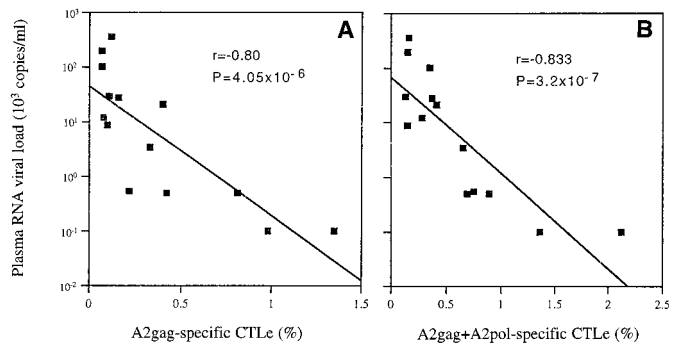


**Fig. 1.** Analysis of PBMCs for the expression of cell surface markers with a FACS Calibur (Becton Dickinson) and CellQuest software (Becton Dickinson). Antibody to CD38 (anti-CD38)-fluorescein isothiocyanate (Dako) and anti-CD8-Tricolor (Caltag) were used according to standard protocols. Briefly, 10<sup>6</sup> PBMCs were centrifuged at 300g for 5 min and resuspended in 50  $\mu$ l of cold phosphate-buffered saline. Tri-color analysis was performed with tetramer-phycoerythrin, anti-CD8-Tricolor, and anti-CD38. The cells were incubated with tetramer and antibodies on ice for 30 to 60 min and then washed twice before formaldehyde fixation. Gates were applied to contain >99.98% of control samples. Controls included both A\*0201-negative individuals and A\*0201-positive HIV-1-uninfected donors. (A to C) CD8<sup>+</sup> T cells from three HIV-1-infected individuals with staining for CD38 along the x axes and for B\*3501-Env tetrameric complex, A\*0201-Gag, and A\*0201-Pol along the y axes, respectively. The tetramer-positive cells make up 0.2 to 2.7% of all CD8<sup>+</sup> cells (values are indicated in each plot) and are all CD38<sup>+</sup>. (D) Comparison of the percentage of CD8<sup>+</sup> cells staining with tetramer and the uncultured peptide-specific cytolytic activity of PBMCs. Each experiment was performed in triplicate. Donors were all HLA A\*0201-positive and were either untreated or treated with combination antiretroviral therapy. Responses to three epitopes were measured [A2Gag, A2Pol, A2EBV BMLF1 280-8 GLCTLVAML (27)] and were all included in the data. Subgroup analyses gave identical results, namely, a significant positive correlation (Pearson correlation coefficient) between percentage peptide-specific lysis and percentage of CD8<sup>+</sup> T cells staining with each tetramer. By multiple stainings on single samples, we have found tetramer binding to be highly reproducible with variation of less than 5% between stains.

**Fig. 2.** Association between plasma RNA viral load and the percentage of CD8<sup>+</sup> cells staining with (A) A2Gag tetramer alone and (B) A2Gag and A2Pol tetramers.



load in 14 HLA A\*0201-positive untreated individuals at different stages of disease (Fig. 2A) and found a highly significant inverse correlation (Pearson correlation coefficient  $r = -0.80$ ,  $P = 4.05 \times 10^{-6}$ ). The addition of A2Gag and A2Pol responses improved the  $P$  value to  $3.2 \times 10^{-7}$  (Fig. 2B). The CD4 counts ranged from 235 to 711 cells/ $\mu$ l (median, 457 cells/ $\mu$ l), and viral load from <500 to 359,500 copies per milliliter (median, 10,418 copies per milliliter). No correlation was detected between CD4 count and viral load or between CD4 count and the circulating HIV-specific A\*0201-restricted CTL activity. Such a lack of associa-

tion between total CD4 count and circulating CTL activity has been reported previously (7, 10, 11, 24).

On the basis of previous calculations, many of those individuals with sufficient circulating HIV-specific CTLs to have fresh HIV-specific cytolytic activity will lyse target cells with half-lives of less than 1 day (7, 8). For a cytopathic virus (short half-life of infected cells), CTL-mediated lysis would be unlikely to significantly further shorten the half-life of infected cells while still causing the death of most infected cells. A small change in the lifespan of productively infected cells may have a large effect on viral burst size. In

REFERENCES AND NOTES

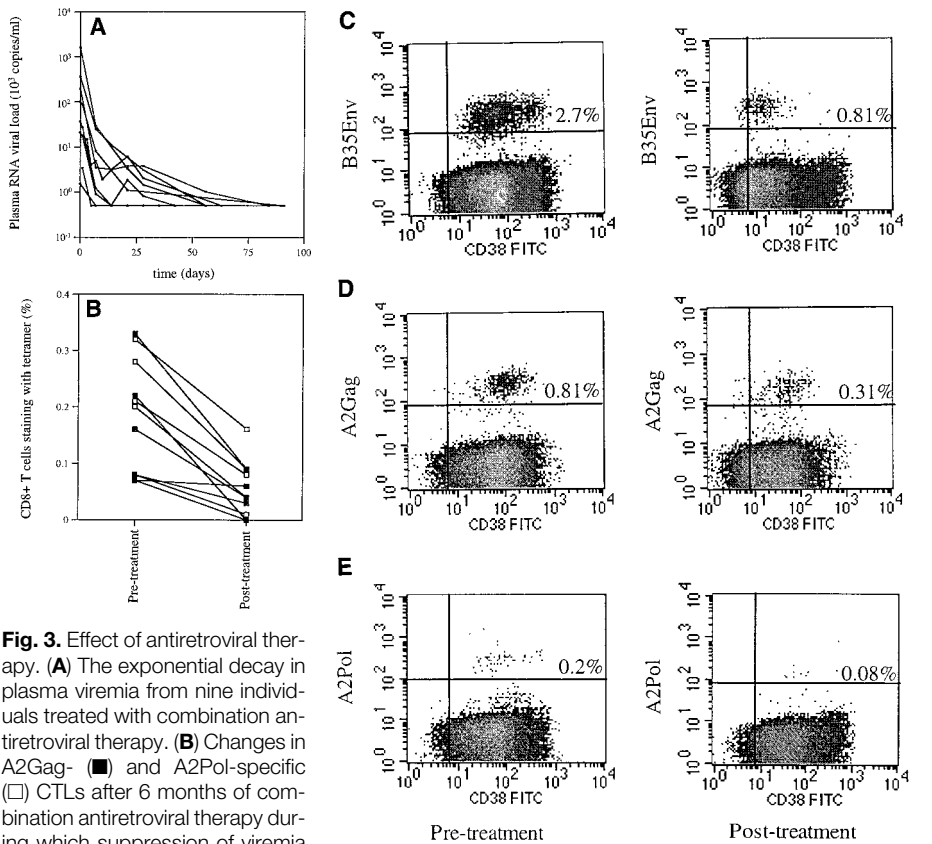


**Fig. 3.** Effect of antiretroviral therapy. **(A)** The exponential decay in plasma viremia from nine individuals treated with combination antiretroviral therapy. **(B)** Changes in A2Gag- (■) and A2Pol-specific (□) CTLs after 6 months of combination antiretroviral therapy during which suppression of viremia was maintained. **(C to E)** Changes in B35Env (C), A2Gag (D), and A2Pol (E) staining of PBMCs from three individuals before and after 6 months of therapy. The x axes show staining with anti-CD38, and the y axes staining with tetramer. The values in each plot are the percentage of CD8<sup>+</sup> T cells staining with the relevant tetramer. Before treatment, the plasma RNA viral loads were 46500, 1420, and 27720 copies per milliliter, respectively. After 6 months of therapy all three individuals had plasma RNA viral loads below the levels of detection.

contrast, for a noncytopathic virus, CTL-mediated lysis would significantly shorten the otherwise relatively long half-life of infected cells. Thus, if the virus is cytopathic, CTL-mediated lysis should reduce RNA viral load while having minimal effect on the clearance rate of infected cells. We examined this hypothesis in 9 of the 14 individuals who received triple-combination therapy shortly after the CTL measurements were made. The subsequent decline in plasma viral RNA was used to derive the exponential clearance rate of productively infected cells (25) (Fig. 3A). The clearance rate did not correlate with the percentage of A2Gag or A2Pol staining or with CD4 count, confirming that the decline in productively infected cells was independent of disease stage (CD4 count) or immune status of the patients.

To examine whether the inverse association of HIV-specific CTLs and plasma RNA viral load was due to suppression of the virus by CTLs and not vice versa, we artificially reduced viral load using triple-combination antiretroviral therapy. The nine treated individuals were studied again at 6 months

after starting treatment when all had viral loads below the detectable limit (<500 copies per milliliter). At 6 months after starting therapy, a new steady state will have been reached, thus eliminating the rapid early fluctuations in the CD8 population observed in previous studies (26). In all cases, we observed a decrease in the HIV-specific CTLs and consistent with the dependence of HIV-specific CTLs on continued viral replication (Fig. 3, C to E).

Using HLA-tetrameric complexes, we have demonstrated a significant inverse association between A\*0201-restricted HIV-specific CTLs and plasma RNA viral load. No significant correlation was detected between the A\*0201-restricted HIV-specific CTLs and CD4 count or clearance rate of productively infected cells. These findings strongly support the involvement of CTLs in the control of HIV infection. Furthermore, these data add weight to the search for a vaccine or therapeutic strategies designed to boost the HIV-specific CTL response.

1. J. W. Mellors *et al.*, *Ann. Intern. Med.* **122**, 573 (1995); J. W. Mellors *et al.*, *Science* **272**, 1167 (1996); J. W. Mellors *et al.*, *Ann. Intern. Med.* **126**, 946 (1997); T. R. O'Brien *et al.*, *J. Am. Med. Assoc.* **276**, 105 (1996).
2. R. A. Koup *et al.*, *J. Virol.* **68**, 4650 (1994).
3. P. Borrow *et al.*, *ibid.*, p. 6103.
4. R. E. Phillips *et al.*, *Nature* **354**, 453 (1991).
5. S. Koenig *et al.*, *Nature Med.* **1**, 330 (1995); P. Borrow *et al.*, *ibid.* **3**, 205 (1997); D. A. Price *et al.*, *Proc. Natl. Acad. Sci. U.S.A.* **94**, 1890 (1997); P. J. R. Goulder *et al.*, *Nature Med.* **3**, 212 (1997).
6. C. M. Walker *et al.*, *Science* **234**, 1563 (1986); F. Cocchi *et al.*, *ibid.* **270**, 1811 (1995).
7. P. Klenerman *et al.*, *Proc. Natl. Acad. Sci. U.S.A.* **93**, 15323 (1996).
8. S. Bonhoeffer *et al.*, *ibid.* **94**, 6971 (1997); M. A. Nowak and C. R. M. Bangham, *Science* **272**, 74 (1996).
9. M. D. Grant *et al.*, *AIDS* **6**, 1085 (1992).
10. C. R. Rinaldo *et al.*, *AIDS Res. Hum. Retroviruses* **11**, 481 (1995).
11. T. C. Greenough *et al.*, *J. Infect. Dis.* **176**, 118 (1997).
12. Y. Cao *et al.*, *N. Engl. J. Med.* **332**, 201 (1995); T. Harrer *et al.*, *J. Immunol.* **156**, 2616 (1996); C. Rinaldo *et al.*, *J. Virol.* **69**, 5838 (1995); M. R. Klein *et al.*, *J. Exp. Med.* **181**, 1365 (1995); K. Ariyoshi *et al.*, *AIDS* **9**, 555 (1995).
13. L. Musey *et al.*, *N. Engl. J. Med.* **337**, 1267 (1997).
14. F. M. Gotch *et al.*, *Int. Immunol.* **2**, 707 (1990); P. A. H. Moss *et al.*, *Proc. Natl. Acad. Sci. U.S.A.* **92**, 5773 (1995).
15. J. D. Altman *et al.*, *Science* **274**, 94 (1996); G. S. Ogg *et al.*, in preparation; P. R. Dunbar *et al.*, in preparation.
16. Complexes were synthesized as described (13). Briefly, purified HLA heavy chain and  $\beta_2M$  were synthesized by means of a prokaryotic expression system (pET R+D). The heavy chain was modified by deletion of the transmembrane-cytosolic tail and COOH-terminal addition of a sequence containing the BirA enzymatic biotinylation site (3' primer for HLA B\*3501, GGAGTGGGACTC-TACCCTCGGTCCTAGGGACGTAGTATAAGACCTA-CGTGTCTTTTACCACACCTTAGTAGCAATTCGAA-TAGTGT). Heavy chain,  $\beta_2M$ , and peptide were refolded by dilution. The 45-kD refolded product was isolated by fast protein liquid chromatography and then biotinylated by BirA in the presence of biotin (Sigma), adenosine 5'-triphosphate (Sigma), and  $Mg^{2+}$  (Sigma). Streptavidin-phycoerythrin conjugate (Leinco) was added in a 1:4 molar ratio, and the tetrameric product was concentrated to 1 mg/ml.
17. H. Shiga *et al.*, *AIDS* **10**, 1075 (1996).
18. K. C. Parker *et al.*, *J. Immunol.* **149**, 3580 (1992).
19. T. J. Tsomides *et al.*, *Proc. Natl. Acad. Sci. U.S.A.* **88**, 11276 (1991).
20. Abbreviations for the amino acid residues are as follows: A, Ala; C, Cys; D, Asp; E, Glu; F, Phe; G, Gly; H, His; I, Ile; K, Lys; L, Leu; M, Met; N, Asn; P, Pro; Q, Gln; R, Arg; S, Ser; T, Thr; V, Val; W, Trp; and Y, Tyr.
21. Elispot assays were done as described [A. Lalvani *et al.*, *J. Exp. Med.* **186**, 859 (1997)]. Briefly, Elispot plates (Millipore) were coated with antibody to human IFN- $\gamma$  overnight (Mabtech). The plates were washed six times and incubated for 1 hour with RPMI 1640 and 5% human serum. Target cells (T2) prepulsed with 1  $\mu$ M epitope peptide were plated at  $10^4$  cells per well. Effector cells were added directly from a fluorescent-activated cell sorter (FACS) sort (FACS Vantage) and incubated for 48 hours at 37°C and 5% CO<sub>2</sub>. The cells were removed, and the plates developed with a second antibody to human IFN- $\gamma$  (biotinylated) and streptavidin-alkaline phosphatase (Mabtech). Fresh cytotoxicity assays were done in triplicate as follows. A\*0201- or B\*3501-matched Epstein-Barr virus (EBV)-transformed B cell lines were incubated at 37°C for 1 hour in the presence of Na<sub>2</sub><sup>51</sup>CrO<sub>4</sub> (Amersham) at 2  $\mu$ Ci/ $\mu$ l. The cells were washed once in medium containing 10% fetal calf serum and incubated either with or without peptide at 1  $\mu$ M for 1 hour. The targets were washed further two times before plating into 96-well round-bottomed plates at 2500 cells per well. A volume of 100  $\mu$ l

containing  $2.5 \times 10^5$  PBMCs was added to each well after counting in the presence of trypan blue. The plates were incubated at 37°C for 4 hours before harvesting 20  $\mu$ l of supernatant. Percentage lysis was estimated as [(experimental counts – media control)  $\times$  100]/(detergent counts – media control). Lysis of non-peptide controls was subtracted to give peptide-specific lysis. Media controls were between 10 to 15% of detergent controls.

22. One tetramer-positive CD8<sup>+</sup> cell was cloned directly into each well of a 96-well flat-bottomed plate (Nunc) in

the presence of  $10^6$  irradiated PBMCs from at least three donors, together with phytohemagglutinin (5  $\mu$ g/ml, Wellcome) in RPMI 1640 (Gibco) supplemented with glutamine, penicillin, streptomycin, and 5% human serum. After 4 days, Lymphocult-T (Biotest) was added to a final concentration of 10%. After 3 weeks the cultures were expanded into 24-well plates.

23. P. J. R. Goulder *et al.*, *J. Exp. Med.* **185**, 1423 (1997).  
24. A. Carmichael *et al.*, *ibid.* **177**, 249 (1993).  
25. D. D. Ho *et al.*, *Nature* **373**, 123 (1995); X. Wei *et al.*, *ibid.*, p. 117.

26. B. Autran *et al.*, *Science* **277**, 112 (1997).  
27. N. Steven *et al.*, *J. Exp. Med.* **185**, 1605 (1997).  
28. The assistance of the nursing staff at Rockefeller Hospital and of J. Jin and J. Song in processing PBMC samples is gratefully acknowledged. Supported by grants from NIH (U01AI41534) and General Clinical Research Center (GCRC) (MO1-RR00102). G.S.O., P.R.D., V.C., S.L.R.-J., and A.J.M. are funded by the Medical Research Council (UK). S.B. and N.A.M. are supported by the Wellcome Trust.

25 November 1997; accepted 29 January 1998

## Biodiversity Assessment and Conservation Strategies

Albert S. van Jaarsveld,\* Stefanie Freitag, Steven L. Chown, Caron Muller, Stephanie Koch, Heath Hull, Chuck Bellamy, Martin Krüger, Sebastian Endrödy-Younga, Mervyn W. Mansell, Clarke H. Scholtz

The efficient representation of all species in conservation planning is problematic. Often, species distribution is assessed by dividing the land into a grid; complementary sets of grids, in which each taxon is represented at least once, are then sought. To determine if this approach provides useful surrogate information, species and higher taxon data for South African plants and animals were analyzed. Complementary species sets did not coincide and overlapped little with higher taxon sets. Survey extent and taxonomic knowledge did not affect this overlap. Thus, the assumptions of surrogacy, on which so much conservation planning is based, are not supported.

Practical conservation uses surrogate information, such as richness of indicator taxa, endemism (taxa restricted to a given area), or higher taxon richness (that is, genus or family richness) to identify possible conservation areas (1–8). Although not universally accepted (9), there is broad agreement that conservation areas should strive to sample regional features, a goal that is most efficiently accomplished with complementary sets (10, 11). These are sets of grids that contain all species in a taxon at least once (10, 12); the complementarity principle ensures that conservation areas represent all species efficiently and that rare species are included (10). Although the outcome of such a complementarity analysis provides a sound basis for the efficient conservation of the focal taxon, it is commonly assumed that the outcome is more widely applicable to other taxa (13).

The value of species richness, species

rarity, and higher taxon richness as biodiversity surrogate measures (“traditional” surrogates) has been explored, and the consensus is that richness “hotspots” (highly species-rich areas) and “coldspots” (areas poor in species) rarely coincide; nor do hotspots and rare (restricted range) taxa generally coincide (6, 14–17). However, the surrogacy value of complementary sets has not been assessed. Here, the relation between traditional surrogate measures and complementary sets, as well as the degree of overlap among complementary sets across taxa, is investigated.

The study incorporated 9119 species, including well-studied taxa that are frequently used as biodiversity indicators (4), such as vascular plants (Plantae), mammals (Mammalia), birds (Aves), and butterflies (Hesperioidea and Papilionoidea), and less well-known taxa, such as termites (Isoptera), antlions (Myrmeleontidae), buprestid beetles (Buprestidae), and scarabaeoid beetles (Scarabaeoidea) (18). These taxa vary considerably with regard to survey extent and taxonomic knowledge. For example, birds are surveyed in all grid cells and all species are included, whereas ~20% of antlion species are included and these are surveyed in 8% of the grid cells in the study area. Species that were chosen for inclusion in the poorly surveyed taxa represent either the known fauna for the region (for example, buprestids and

scarabs) or, where the majority of the fauna has not been adequately cataloged, a well-known monophyletic unit (antlions). In one instance (termites), only an incomplete set of published data from a systematic survey was available, resulting in poor species coverage (19). In none of these cases was there reason to presume that the species chosen are a nonrandom subset of the taxon as a whole with regard to geographic distribution.

Data from the Transvaal region (now including Gauteng, Mpumalanga, Northern, and part of North-West provinces; South Africa) were mapped on a 25 km by 25 km grid ( $n = 474$ ), and complementary sets for each of the taxa were identified by means of a rarity-based algorithm (12). The study area is about the size of the United Kingdom and comprises 20% of the surface area of one of the most species-rich countries in the world. Richness hotspots and coldspots reflect the top 5% of species-rich and species-poor 25-km squares, respectively (14). Rare species are defined as those occurring in less than 24 squares (5% of 474 squares), and this rarity may be the consequence of a restricted range or inadequate sampling (20). The degree of spatial overlap among complementary sets, species richness (hotspots and coldspots), and areas containing rare taxa is expressed by the Jaccard coefficient (Table 1).

As in previous studies (14), we found little overlap within taxa using measures of richness (hotspots and coldspots) and rarity (21) (Fig. 1 and Table 1). The single exception was richness hotspots and rarity where the mean overlap was 50% (Table 1). This high value was due mostly to high overlap values in plants and in phytophagous insects (plants, buprestids, and butterflies all had overlap values exceeding 75%) (Table 1). Speciose plant regions in southern Africa include large numbers of rare plant species (22), and patterns in plant diversity are often a good predictor of patterns in insect diversity (23). This may account, at least to some extent, for the high overlap values of richness hotspots and rarity observed within each of these taxa.

Overlap among taxa for richness hotspots and coldspots is, respectively, highest between butterflies and plants (24%), and scarab and buprestid beetles (13%) (24). Overlap among areas containing rare taxa is most

A. S. van Jaarsveld, S. Freitag, S. L. Chown, C. Muller, S. Kock, H. Hull, C. H. Scholtz, Department of Zoology and Entomology, University of Pretoria, Pretoria 0002, South Africa.

C. Bellamy, M. Krüger, S. Endrödy-Younga, Transvaal Museum, Post Office Box 413, Pretoria 0001, South Africa.

M. W. Mansell, Plant Protection Research Institute, Agricultural Research Council, Private Bag X134, Pretoria 0001, South Africa.

\*To whom correspondence should be addressed. E-mail: albert@scientia.up.ac.za.